Picosecond-resolution fluorescence lifetime imaging microscopy: a useful tool for sensing molecular interactions *in vivo* via FRET

Wei Zhong[1], Mei Wu[2, 3], Ching-Wei Chang[1], Karl A. Merrick[2], Sofia D. Merajver[2, 3], and Mary-Ann Mycek[1, 3, 4 *]

Dept. of Biomedical Engineering[1], Department of Internal Medicine, Division of Hematology and Oncology[2], Comprehensive Cancer Center[3], Applied Physics Program[4], University of Michigan, Ann Arbor, MI 48109-2099
Corresponding author: mycek@umich.edu

Abstract: Fluorescence lifetime imaging microscopy (FLIM) provides a promising, robust method of detecting molecular interactions *in vivo* via fluorescence / Förster resonance energy transfer (FRET), by monitoring the variation of donor fluorescence lifetime, which is insensitive to many artifacts influencing convential intensity-based measurements, e.g. fluorophore concentration, photobleaching, and spectral bleed-through. As proof of principle, we demonstrate the capability of a novel picosecond-resolution FLIM system to detect molecular interactions in a well-established FRET assay. We then apply the FLIM system to detect the molecular interaction of a transforming oncogene RhoC with a binding partner RhoGDIγ *in vivo*, which is critical to understand and interfere with Rho signaling for cancer therapeutics.

OCIS codes: (170.1530) Cell analysis; (170.2520) Fluorescence microscopy; (170.3650) Lifetime-based sensing; (170.4580) Optical diagnostics for medicine; (170.6920) Time-resolved imaging.

References and links

1. P. Legrain and L. Selig, "Genome-wide protein interaction maps using two-hybrid systems," FEBS Lett. **480**, 32-36 (2000).
2. S. Fields, "Proteomics in genomeland," Science **291**, 1221-1224 (2001).
3. E. Golemis, ed., *Protein-protein interactions: A molecular cloning manual*, 1st ed. (Cold Spring Harbor Laboratory Press, Woodbury, 2001), p. 682.
4. Y. Chen and J. D. Mills, "Protein localization in living cells and tissues using FRET and FLIM," Differentiation **71**, 528-541 (2003).
5. K. L. van Golen, Z.-F. Wu, X. T. Qiao, L. W. Bao, and S. D. Merajver, "RhoC GTPase, a novel transforming oncogene for human mammary epithelial cells that partially recapitulates the inflammatory breast cancer phenotype," Cancer Res. **60**, 5832-5838 (2000).
6. H. Suwa, G. Ohshio, T. Imamura, G. Watanabe, S. Arii, M. Imamura, S. Narumiya, H. Hiai, and M. Fukumoto, "Overexpression of the RhoC gene correlates with progression of ductal adenocarcinoma of the pancreas," Br. J. Cancer **77**, 147-152 (1998).
7. E. A. Clark, T. R. Golub, E. S. Lander, and R. O. Hynes, "Genomic analysis of metastasis reveals an essential role for RhoC," Nature **406**, 532-535 (2000).
8. G. Fritz, C. Brachetti, F. Bahlmann, M. Schmidt, and B. Kaina, "Rho GTPases in human breast tumours: expression and mutation analyses and correlation with clinical parameters," Br. J. Cancer **87**, 635-644 (2002).
9. W. B. Zhong, C. Y. Wang, T. C. Chang, and W. S. Lee, "Lovastatin induces apoptosis of anaplastic thyroid cancer cells via inhibition of protein geranylgeranylation and de novo protein synthesis," Endocrinology **144**, 3852-3859 (2003).
10. C. Marionnet, C. Lalou, K. Mollier, M. Chazal, G. Delestaing, D. Compan, O. Verola, C. Vilmer, J. Cuminet, L. Dubertret, and N. Basset-Seguin, "Differential molecular profiling between skin carcinomas reveals four newly reported genes potentially implicated in squamous cell carcinoma development," Oncogene **22**, 3500-3505 (2003).
11. W. Wang, L. Y. Yang, G. W. Huang, and W. Q. Lu, "Expression and significance of RhoC gene in hepatocellular carcinoma," World Journal of Gastroenterology **9**, 1950-1953 (2003).
12. R. Y. Tsien, "The green fluorescent protein," Annual Reviews of Biochemistry **67**, 509-544 (1998).

#88805 - $15.00 USD Received 19 Oct 2007; revised 13 Dec 2007; accepted 14 Dec 2007; published 19 Dec 2007

13. A. Periasamy, "Fluorescence resonance energy transfer microscopy: a mini review," J. Biomed. Opt. **6**, 287-291 (2001).
14. F. J. M. van Kuppeveld, W. J. G. Melchers, P. H. G. M. Willems, and T. W. J. Gadella, Jr., "Homomultimerization of the coxsackievirus 2B protein in living cells visualized by fluorescence resonance energy transfer microscopy," J. Virol. **76**, 9446-9456 (2002).
15. M. Elangovan, R. N. Day, and A. Periasamy, "Nanosecond fluorescence resonance energy transfer-fluorescence lifetime imaging microscopy to localize the protein interactions in a single living cell," J. Microsc. **205**, 3-14 (2002).
16. A. Tsuji, Y. Sato, M. Hirano, T. Suga, H. Koshimoto, T. Taguchi, and S. Ohsuka, "Development of a time-resolved fluorometric method for observing hybridization in living cells using fluorescence resonance energy transfer," Biophys. J. **81**, 501-515 (2001).
17. J. R. Lakowicz, *Principles of Fluorescence Spectroscopy*, 2nd ed. (Kluwer Academic/Plenum, New York, 1999), p. 698.
18. P. I. H. Bastiaens and A. Squire, "Fluorescence lifetime imaging microscopy: spatial resolution of biochemical processes in the cell," Trends Cell Biol. **9**, 48-52 (1999).
19. J. A. Schmid and H. H. Sitte, "Fluorescence resonance energy transfer in the study of cancer pathways," Curr. Opin. Oncol. **15**, 55-64 (2003).
20. P. K. Urayama and M.-A. Mycek, "Fluorescence lifetime imaging microscopy of endogenous biological fluorescence," in *Handbook of Biomedical Fluorescence*, M.-A. Mycek and B. W. Pogue, eds. (Marcel-Dekker Inc., New York, New York, 2003), pp. 211-236.
21. J. Lippincott-Schwartz, E. Snapp, and A. Kenworthy, "Studying protein dynamics in living cells," Nat. Rev. Mol. Cell Biol. **2**, 444-456 (2001).
22. W. Zhong, P. Urayama, and M.-A. Mycek, "Imaging fluorescence lifetime modulation of a ruthenium-based dye in living cells: the potential for oxygen sensing," J. Phys. D: Appl. Phys. **36**, 1689-1695 (2003).
23. C. W. Chang, D. Sud, and M. A. Mycek, "Fluorescence Lifetime Imaging Microscopy," in *Methods in Cell Biology, Vol. 81 - Digital Microscopy, 3rd Edition*, D. E. Wolf and G. Sluder, eds. (Academic Press, San Diego, 2007), pp. 495-524.
24. I. Bugiel, K. König, and H. Wabnitz, "Investigation of cell by fluorescence laser scanning microscopy with subnanosecond time resolution," Lasers in the Life Sciences **3**, 47-53 (1989).
25. X. F. Wang, A. Periasamy, B. Herman, and D. Coleman, "Fluorescence lifetime imaging microscopy (FLIM): Instrumentation and applications," Crit. Rev. Anal. Chem. **23**, 369-395 (1992).
26. T. French, P. T. C. So, C. Y. Dong, K. M. Berland, and E. Gratton, "Fluorescence lifetime imaging techniques for microscopy," Methods Cell Biol. **56**, 277-304 (1998).
27. T. W. J. Gadella, Jr., "Fluorescence lifetime imaging microscopy (FLIM): instrumentation and application," in *Fluorescent and luminescent probes for biological activity*, W. T. Mason, ed. (Academic Press, San Diego, 1999), pp. 467-479.
28. P. J. Tadrous, "Methods for imaging the structure and function of living tissues and cells: 2. fluorescence lifetime imaging," J. Pathol. **191**, 229-234 (2000).
29. R. Cubeddu, D. Comelli, C. D'Andrea, P. Taroni, and G. Valentini, "Time-resolved fluorescence imaging in biology and medicine," J. Phys. D: Appl. Phys. **35**, R61-R76 (2002).
30. P. K. Urayama, W. Zhong, J. A. Beamish, F. K. Minn, R. D. Sloboda, K. H. Dragnev, E. Dmitrovsky, and M.-A. Mycek, "A UV-visible fluorescence lifetime imaging microscope for laser-based biological sensing with picosecond resolution," Applied Physics B: Lasers and Optics **76**, 483-496 (2003).
31. H. J. Lin, P. Herman, and J. R. Lakowicz, "Fluorescence lifetime-resolved pH imaging of living cells," Cytometry A **52**, 77-89 (2003).
32. P. K. Urayama, J. A. Beamish, F. K. Minn, E. A. Hamon, and M.-A. Mycek, "A UV fluorescence lifetime imaging microscope to probe endogenous cellular fluorescence," presented at the Conference on Lasers and Electro-Optics, 2002.
33. X. F. Wang, T. Uchida, D. M. Coleman, and S. Minami, "A two-dimensional fluorescence lifetime imaging system using a gated image intensifier," Appl. Spectrosc. **45**, 360-366 (1991).
34. K. K. Sharman, A. Periasamy, H. Ashworth, J. N. Demas, and N. H. Snow, "Error analysis of the rapid lifetime determination method for double-exponential decays and new windowing schemes," Anal. Chem. **71**, 947-952 (1999).
35. M.-A. Mycek, P. K. Urayama, K. Heyman, and M. Bussey, "Using POPOP's viscosity dependent lifetime as a picosecond resolution standard in near-UV fluorescence lifetime imaging microscopy," Proc. SPIE **4962**, 143-150 (2003).
36. C. J. Grauw and H. C. Gerritsen, "Multiple time-gate module for fluorescence lifetime imaging," Appl. Spectrosc. **55**, 670-678 (2001).
37. H. C. Gerritsen, M. A. H. Asselbergs, A. V. Agronskaia, and W. G. J. H. M. Van Sark, "Fluorescence lifetime imaging in scanning microscopes: acquisistion speed, photon economy and lifetime resolution," J. Microsc. **206**, 218-224 (2002).
38. M. Tramier, I. Gautier, T. Piolot, S. Ravalet, K. Kemnitz, J. Coppey, C. Durieux, V. Mignotte, and M. Coppey-Moisan, "Picosecond-hetero-FRET microscopy to probe protein-protein interactions in live cells," Biophys. J. **83**, 3570-3577 (2002).
39. M. A. Rizzo, G. H. Springer, B. Granada, and D. W. Piston, "An improved cyan fluorescenct protein variant useful for FRET," Nat. Biotechnol. **22**, 445-449 (2004).
40. R. Rose, M. Weyand, M. Lammers, T. Ishizaki, M. R. Ahmadian, and A. Wittinghofer, "Structural and mechanistic insights into the interaction between Rho and mammalian Dia," Nature **435**, 513-518 (2005).

#88805 - $15.00 USD Received 19 Oct 2007; revised 13 Dec 2007; accepted 14 Dec 2007; published 19 Dec 2007

41. P. Madaule, T. Furuyashiki, T. Reid, T. Ishizaki, G. Watanabe, N. Morii, and S. Narumiya, "A novel partner for the GTP-bound forms of rho and rac," FEBS Lett. **377**, 243-248 (1995).
42. A. K. Hadjantonakis and A. Nagy, "The color of mice: in the light of GFP-variant reporters," Histochem. Cell Biol. **115**, 49-58 (2001).
43. G. Feng, R. H. Mellor, M. Bernstein, C. Keller-Peck, Q. T. Nguyen, M. Wallace, J. M. Nerbonne, J. W. Lichtman, and J. R. Sanes, "Imaging neuronal subsets in transgenic mice expressing multiple spectral variants of GFP," Neuron **28**, 41-51 (2000).
44. J. A. Brewer, B. P. Sleckman, W. Swat, and L. J. Muglia, "Green fluorescent protein-glucocorticoid receptor knockin mice reveal dynamic receptor modulation during thymocyte development," J. Immunol. **169**, 1309-1318 (2002).
45. F. Schaufele, I. Demarco, and R. N. Day, "FRET imaging in the wide-field microscope," in *Molecular imaging: FRET microscopy and spectroscopy*, A. Periasamy and R. N. Day, eds. (Oxford University Press, New York, 2005), pp. 72-94.
46. J. Zhang, R. E. Campbell, A. Y. Ting, and R. Y. Tsien, "Creating new fluorescent probes for cell biology," Nat. Rev. Mol. Cell Biol. **3**, 906-918 (2002).
47. G. Valentin, C. Verheggen, T. Piolot, H. Neel, M. Coppey-Moisan, and E. Bertrand, "Photoconversion of YFP into a CFP-like species during acceptor photobleaching FRET experiments," Nat Methods **2**, 801 (2005).
48. C. Thaler, S. S. Vogel, S. R. Ikeda, and H. Chen, "Photobleaching of YFP does not produce a CFP-like species that affects FRET measurements," Nat Methods **3**, 491; author reply 492-493 (2006).
49. S. E. Verrier and H. D. Soling, "Photobleaching of YFP does not produce a CFP-like species that affects FRET measurements," Nat Methods **3**, 491-492; author reply 492-493 (2006).
50. R. Reddel, Y. K. Ke, V. Gerwin, M. McMenamin, J. Lechner, R. Su, D. Brash, J.-B. Park, J. Limb Rhim, and C. Harris, "Transformation of human bronchial epithelial cells by infections by SV40 or adenovius-12 SV40 hybrid virus, or transfection via strontium phosphate coprecipitation with the plasmid containing SV40 early region genes," Cancer Res. **48**, 1904-1909 (1988).
51. A. W. Nguyen and P. S. Daugherty, "Evolutionary optimization of fluorescent proteins for intracellular FRET," Nat. Biotechnol. **23**, 355-360 (2005).
52. O. Griesbeck, G. S. Baird, R. E. Campbell, D. A. Zacharias, and R. Y. Tsien, "Reducing the environmental sensitivity of yellow fluorescent protein. Mechanism and applications," J. Biol. Chem. **276**, 29188-29194 (2001).

1. Introduction

The ability to rapidly characterize molecular function *in vivo* would be a fundamental advance in biology and medicine. Traditional biophysical or biochemical methods, such as affinity chromatography or co-immunoprecipitation, and more recently, two-hybrid and phage-display methods have been used to detect molecular interactions *in vitro* [1-4]. However, many molecular interactions require integrity of the cell's metabolic machinery and molecular transport within the cell, so that they may be undetectable *in vitro* by techniques which do not preserve living cells. Moreover, biologically important molecules that exist in more than one activation state are hard to isolate from the complex *in vivo* system while preserving the integrity of their activation cycle. One such molecule, RhoC, has been found to be a transforming oncogene. RhoC enhances cell motility, angiogenesis, and metastasis when activated [5-11]. However, the biophysical mechanisms for activation and inhibition of this oncogene (including detailed molecular associations and cellular localization) are not well understood in part due to the limitations of traditional biophysical and biochemical methods.

FRET can detect biomolecular interactions with high spatial sensitivity in living cells and is therefore considered a useful means of studying molecular interactions [12-16]. FRET is a quantum mechanical process involving the nonradiative transfer of energy between fluorophores (i.e. donor and acceptor pairs) that occurs when an excited donor molecule dipole couples to an acceptor molecule [17]. Conditions affecting FRET efficiency include proximity of the donor-acceptor pair (typically 1 to 10 nm), relative orientation, and spectral overlap between the donor's emission spectrum and the acceptor's excitation spectrum, which has been described mathematically [15, 17, 18]. Based on this physical understanding of FRET, it is possible to use FRET measurements as extremely sensitive nanoscale "rulers" by which specific molecular interactions are detected.

FRET can be observed by monitoring fluorescence emission from either the donor or the acceptor [13, 15-18]. If the donor is monitored, FRET will lead to a decrease in fluorescence emission intensity and electronic excited state lifetime of the donor when the acceptor in close

#88805 - $15.00 USD Received 19 Oct 2007; revised 13 Dec 2007; accepted 14 Dec 2007; published 19 Dec 2007

proximity quenches the donor fluorescence. Conversely, if the acceptor is monitored, FRET will lead to an increase in fluorescence intensity and lifetime of the acceptor as the excited-state reaction between donor and acceptor leads to a rise time in the acceptor decay kinetics [17].

Some pioneering studies on FRET were carried out by intensity-based methods [19]. However, artifacts influencing fluorescence intensity in biological systems were prominent. These included fluorophore concentration, photobleaching, and sources of optical loss (absorption and scattering), all of which hamper the correct and reliable interpretation of the fluorescence intensity of the emission of an acceptor [19, 20]. Moreover, spectral bleed-through (due to the overlap of the emission spectra of a donor and an acceptor as well as direct excitation of the acceptor by excitation light for the donor) may lead to false positive FRET images [19]. To minimize or eliminate some of these artifacts, many methods were developed to calculate correction factors, but some of these methods are vulnerable to photobleaching [19, 21]. Nevertheless, most of these methods require extensive calibration involving imaging of different samples (donor only, acceptor only, donor and acceptor) using different combinations of filters for excitation and emission of donor and acceptor [19, 21].

Compared to fluorescence intensity-based methods, lifetime imaging requires less calibration and/or correction for fluorophore concentration, photobleaching and other artifacts that affect intensity measurements [15, 17, 18, 20-23]. Although FRET causes the donor lifetime to decrease and the acceptor lifetime to increase [17], only the donor lifetime was monitored in these experiments because acceptor emission is contaminated by spectral bleed-through [15, 17]. FLIM is a technique that uses fluorophore lifetime rather than fluorescence intensity for image contrast. First reported in 1989 [24], it has been used to probe the microenvironments of endogenous and exogenous fluorophores, including pH, dissolved gas concentration, and molecular interactions [20, 25-31]. It has been employed to detect the donor lifetime change in the absence vs. presence of the acceptor, as evidence of FRET [15, 16, 19, 21, 23]. However, these methods require specific and often expensive instruments.

We have recently designed and characterized a novel wide-field, time-domain fluorescence lifetime imaging microscopy (FLIM) system developed for picosecond time-resolved biological imaging [30]. A nitrogen laser pumping a dye laser for UV-visible-NIR excitation offers a significantly less expensive, wide-field, and importantly for clinical applications, potentially portable alternative to multi-photon excitation for sub-nanosecond FLIM imaging of biological samples [30]. The large temporal dynamic range (750 ps – 1 μs) and the 50 ps lifetime discrimination of the system makes it suitable for studying many endogenous and exogenous fluorophores that may transit through cells [20, 22, 32].

In this article, we describe the FLIM system and method for measuring FRET. Then, we demonstrate the FLIM system's capability of detecting FRET in a well-established FRET assay. Finally, we compare lifetime vs. intensity measurements of donor fluorescence, illustrating the benefit of using lifetime imaging vs. intensity imaging for highly sensitive FRET detection of key biological molecules.

2. Methods

2.1. FLIM system

A wide-field, time-domain FLIM system developed for picosecond biological sensing was described in detail previously [30]. The concept behind the time-domain lifetime determination is illustrated in Fig. 1(a). Briefly, an excitation pulse illuminates a sample and an image of the fluorescence emission is acquired by an intensified charge-coupled device (ICCD) camera at a controllable intensifier gate delay t_G, with emission intensities integrated during the gate width Δt. Fluorescence lifetime images are determined by obtaining fluorescence intensity images at several gate delays and analyzing the fluorescence intensity decay on a pixel-by-pixel basis.

Fig. 1(b) shows the schematic of the FLIM system, with some key experimental specifications for imaging living cells described below. The excitation source consisted of a

#88805 - $15.00 USD Received 19 Oct 2007; revised 13 Dec 2007; accepted 14 Dec 2007; published 19 Dec 2007

pulsed nitrogen laser (GL-3300, Photon Technology International, Lawrenceville, NJ) pumping a dye laser (GL-301, Photon Technology International, Lawrenceville, NJ), with a wavelength range from UV through near infrared (NIR), depending on the dye used. The excitation light was delivered via an optical fiber (SFS600/660N, Fiberguide Industries, Stirling, NJ) to a research-grade, inverted microscope (Axiovert S100 2TV, Zeiss, Germany) in epi-illumination mode.

A reference pulse split from the excitation light via a beam splitter was sent to an optical discriminator to generate an electronic pulse, providing a time reference to a picosecond delay generator (DEL350, Becker & Hickl, Germany). The delay generator output was used to trigger the gated ICCD camera (Picostar HR, LaVision, Germany). The ICCD had variable intensifier gain and gate width settings varying from 200 ps to 10 ms. For lifetime data acquisition, gated images were averaged over 5 laser pulses and showed less than 2% standard deviation in fluorescence intensity.

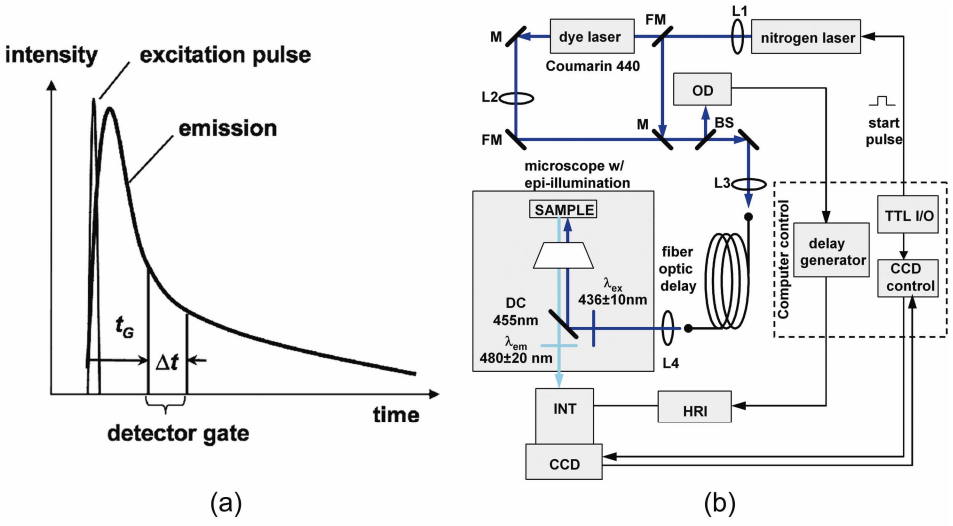

Fig. 1. (a). FLIM concept. The system captures fluorescence intensity image at a time t_G after the excitation pulse over the interval Δt. Lifetime can be created using intensity images captured at several different t_G. (b) FLIM Setup. Excitation light from a nitrogen laser pumping a dye laser (UV-visible-NIR) is delivered by an optical fiber to a microscope. Fluorescence emission is captured by a fast-gated intensified charge-coupled device, which is triggered by a delay generator, using a timing reference provided by a reference pulse split from the excitation light with a beam splitter. Abbreviations: CCD = charge-coupled device; HRI = high rate imager; INT = intensifier; TTL I/O = TTL input/output card; OD = optical discriminator; BS = beam splitter; DC = dichroic mirror; FM = "flippable" mirror; L1, L2, L3, L4 = quartz lenses; M = mirror. Thick solid lines = light path; thin solid line = electronic path.

To create fluorescence lifetime images rapidly, an analytic least squares lifetime determination algorithm was used [24, 33, 34]:

$$\tau_p = -\frac{N(\sum t_i^2) - (\sum t_i)^2}{N\sum t_i \ln I_{i,p} - (\sum t_i)(\sum \ln I_{i,p})}, \quad (1)$$

where τ_p is the lifetime of pixel p, $I_{i,p}$ is the intensity of pixel p in image i, t_i is the gate delay of image i, and N is the number of images. All sums are over i.

The FLIM system's ability to discriminate between samples with different fluorescence lifetimes was determined by measuring solutions of the standard sample 1,4-bis(5-phenyloxazol-2-yl)benzene (POPOP) at different viscosities, produced by varying the ratio of glycerol to ethanol in the mixture [30, 35]. The measured difference of 0.05±0.03 ns between the 80%- and 60%-ethanol samples was confirmed to be statistically significant via a

#88805 - $15.00 USD Received 19 Oct 2007; revised 13 Dec 2007; accepted 14 Dec 2007; published 19 Dec 2007

fluorescence lifetime spectrometer [30, 35]. Therefore, the FLIM system was able to discriminate lifetime differences at least as small as 50 ps [30, 35], making it more than sufficiently sensitive to detect lifetime differences in the following FRET experiments.

2.2. Preparation, imaging, and data analysis of FRET assay in solution

A well-controlled chemical assay - BACE1 (β-Secretase) FRET assay (Part # P2985, PanVera Corporation, Madison, WI) was prepared. The substrate consists of a peptide-linked fluorescence donor (a rhodamine derivative) and quenching acceptor. The intensity and lifetime of fluorescence of the donor increase upon enzymatic cleavage because the resonance energy transfer from the donor to the quenching group is disrupted.

We measured the fluorescence of the BACE1 product standard, which corresponds to the maximum fluorescence intensity and lifetime at the end of the enzymatic reaction, since product standard represents 100% cleavage of the substrate by the enzyme. We then measured the BACE1 substrate fluorescence, which represents the baseline of fluorescence intensity and minimum lifetime. Finally, we mixed BACE1 substrate, BACE1 enzyme, and assay buffer, monitoring the change of fluorescence intensity over time and extracting the lifetime.

All samples above were loaded into capillaries for imaging with a Zeiss Fluar 40X oil-immersion objective. The excitation wavelength was at 540 nm and the emission was collected from 570 – 610 nm. Signals were detected with a neutral density filter (O.D.=0.5) placed after the nitrogen laser, with voltage across the micro-channel plate (MCP) and gate width of the intensifier set at 700 V and 200 ps, respectively.

Four fluorescence intensity images were used for calculating lifetime images, because a four-gate protocol was found to yield more consistent fluorescence lifetime values for repeated measurements, whereas two-gate and three-gate protocols were more sensitive to noise. This is consistent with the results from Monte-Carlo simulations reported in the literature: detection systems equipped with four to eight time-gates were significantly more sensitive than the two time-gate system, but only minor sensitivity differences were found between systems with four or more time-delays [36, 37]. To increase signal-to-noise ratio, each intensity image was binned 4 by 4. The background noise in each intensity image was subtracted before calculating the lifetime image. Residual background noise due to pixel-to-pixel fluctuation is further rejected by setting the intensity value of pixels in the background-corrected intensity images with fewer than 8 camera counts to zero. Any pixel with lifetime longer than 5 ns was rejected in creating the lifetime images. The average lifetime was calculated by averaging the lifetime over all nonzero pixels within a ROI for each sample.

2.3. Maintenance, preparation, and transfection of living cells

Monkey kidney epithelial (CV-1) cells were cultured to 60-75% confluency in MEM (CellGro, Mediatech Incorporated, Herndon, VA) supplemented with 10% FBS (Gibco, Invitrogen Corporation, Carlsbad, California) at 37°C under 5% CO_2. Twenty-four hours before transfection, the cells were trypsinized by first washing with HBSS (BioWhittaker, Cambrex Corporation, East Rutherford, New Jersey) and subsequently adding 1x Trypsin-EDTA solution (CellGro) supplemented with 0.05% Trypsin (BioWhittaker). Trypsin was neutralized using the MEM solution before cells were collected. The concentration of cells in this collection was determined using a hemocytometer and an appropriate volume was aliquoted to yield $2x10^5$ cells per transfection. This aliquot was then centrifuged at 1200 rpm for 4 minutes and the supernatant was removed. The cells were resuspended in MEM (1.5 ml / plate) with 10% FBS and were plated evenly in 35-mm Glass-Bottom Microwell Dishes (MatTek Corporation, Ashland, MA) and incubated for 24 hours at 37°C under 10% CO_2.

The following day, for each transfection, 6 μl of GeneJammer transfection reagent (Stratagene, La Jolla, CA) was added (6 μl / μg DNA) to 100 μl of DMEM I Serum-free medium (Gibco) and allowed to incubate for 10 minutes at room temperature. Following this incubation, 1.5 μg of the enhanced cyan fluorescent protein (ECFP) fusion plasmids and 2.5 μg of the enhanced yellow fluorescent protein (EYFP) fusion plasmids were added to the

#88805 - $15.00 USD Received 19 Oct 2007; revised 13 Dec 2007; accepted 14 Dec 2007; published 19 Dec 2007

transfection mix, which was subsequently allowed to incubate for another 10 minutes at room temperature. After this incubation, the medium from the cells set up on the previous day was removed and the plates were washed with 1ml of MEM. Following this wash, 900 μl of MEM was added to each plate and the transfection mix was added to the plate drop-wise in the microwell. After this, cells were incubated for 3 hours at 37°C under 5% CO_2 and subsequently an additional 1 ml of MEM was added before returning the cells to the incubator where they rested for approximately 24 hours.

Group 1 cells transfected with ECFP-RhoGDIγ fusion plasmids, which expressed fusion proteins of ECFP and RhoGDIγ, and EYFP plasmids, which expressed proteins of EYFP, were used as negative controls because no FRET would occur in the absence of RhoC except for that caused by random collisions between ECFP and EYFP. Group 2 cells transfected with ECFP-RhoGDIγ fusion plasmids and EYFP-RhoC fusion plasmids, which expressed fusion proteins of EYFP and RhoC, were used to study the interaction between RhoGDIγ and RhoC. Determining the appropriate doses of ECFP and EYFP plasmids required some care. The quantity of plasmid transfected was kept at 4 μg to prevent significant cell loss. In order to increase the weak ECFP fluorescence signal, different doses of donor and acceptor fusion plasmids (donor / acceptor: 1 μg / 3μg, 1.5 μg / 2.5 μg, 2 μg / 2 μg) were used to search for the optimal dose that resulted in good signals without significant cell loss. Although increasing the dose of donor fusion plasmid helped to increase donor fluorescence, the effort was compromised by the decrease in the efficiency of FRET, as FRET was most efficient with a stoichiometry favoring the interaction of proteins fused to the donor fluorophores with the proteins fused to the acceptor fluorophores. Based on these considerations, in this system 1.5 μg and 2.5 μg of ECFP and EYFP fusion plasmids were used, respectively. The doses of plasmids containing ECFP and EYFP used to transfect groups 1 and 2 were kept as constant as possible, so that any homodimer formation between ECFP molecules which might cause ECFP lifetime to decrease [38, 39] would be accounted for equally in both groups.

Because another cyan fluorescent protein variant – Cerulean – was reported to have better spectroscopic properties than ECFP [39], groups of cells were transfected with Cerulean fusion plasmids substituting ECFP fusion plasmids, under the same conditions as described above.

2.4. Imaging and data analysis of living cells

The standard MEM was replaced with phenol-red free MEM before imaging to eliminate background fluorescence. Cells that were not transfected were checked with both ECFP (or Cerulean) and EYFP filter sets (31044v2 and 41028, Chroma Technology Corporation, Rockingham, VT) on a Zeiss Axiovert 25 microscope at 10X objective and no autofluorescence was observed visually. Transfected cells were checked with both ECFP and EYFP filter sets to ensure the presence of both ECFP and EYFP fluorescence, indicating the successful transfection of the two types of experimental plasmids into cells. Cells transfected with plasmids containing EYFP were checked to show no fluorescence when the ECFP filter set was used. This is important because contamination of donor fluorescence from acceptor fluorescence would introduce artifacts into this experiment where we seek to detect fluorescence only from donor fluorophores. Transfection efficiency was about 30%.

Cells were imaged with the FLIM system using a Zeiss Fluar 40X oil-immersion objective. ECFP (or Cerulean) fluorescence was excited at λ_{ex} = 436±10 nm using the laser dye Coumarin 440 and collected at λ_{em} = 480±20 nm. A neutral density filter (ND=0.5) was placed at the port where the excitation light enters the microscope to prevent photobleaching. Energy at the sample was about 14 μJ / pulse. Measurements were repeated twice to test reproducibility of the experiments, which was calculated as the half difference in the mean values of two immediately consecutive measurements divided by the average of their mean values. Since different cells in a sample might not be focused at the same optical plane due to differences in morphology, intensity-based measurements require adjusting the focus for each cell. The insensitivity of lifetime measurements to small changes in focus was verified by intentionally changing the objective slightly, thereby eliminating the need for adjusting the

#88805 - $15.00 USD Received 19 Oct 2007; revised 13 Dec 2007; accepted 14 Dec 2007; published 19 Dec 2007

focus for each cell during the experiments. All measurements were done within about 15 minutes to ensure that cells were still healthy throughout.

Intensity images of ECFP fluorescence from living cells were taken at four delay gates, for reasons mentioned under section 2.2. The gate width of the intensifier on the ICCD was set to the minimal 200 ps, which is considered appropriate for studying fluorophores with lifetimes around nanoseconds, such as ECFP and Cerulean. Due to the weak signal strength, the MCP voltage of the intensifier was set at 800 V.

The background noise in each image, measured as the average counts in a region without cells, were subtracted from the intensity images before calculating the lifetime image. Residual background noise due to pixel-to-pixel fluctuation is further rejected by setting the intensity value of pixels in the background-corrected intensity images below a threshold value to zero.

In the lifetime images, each cell was analyzed by defining a minimal ROI enclosing the whole cell. Because background noise was rejected as described above, all the pixels within this rectangle with nonzero values corresponded to signals from cells. The average lifetime of a cell was calculated by averaging the lifetime over all nonzero pixels within the rectangle. An image mask was created by setting the values of those nonzero pixels to 1 in the lifetime image. The image mask was then multiplied by the background-corrected fluorescence intensity image to create the final intensity image, which only has fluorescence signals at pixels where there is a meaningful lifetime value. The average intensity of a cell was calculated by the same method. The mean lifetime and intensity for a group of cells were calculated as the average of the lifetime and intensity values of all the measured individual cells in the group. Cells with very weak mean intensities were excluded, as their lifetimes were heavily skewed by the dominance of noise with intrinsically infinite lifetime. Our results (data not shown) confirmed that above a certain threshold, there is no dependence of mean lifetimes on mean intensities.

2.5. Construction and analysis of tagged RhoC and RhoGDIγ in biochemical assay

The cDNA clones of RhoGDIγ, Myc-tagged RhoA, and HA-tagged RhoC in the vector pcDNA3.1 (Invitrogen Corporation) were purchased from Guthrie cDNA collection (www.cdna.org). The plasmid pcDNA3.1-Myc-RhoGDIγ was constructed as follows: The RhoGDIγ gene was released by digesting the cDNA clone with EcoRI (Roche Diagnostics Corporation, Indianapolis, IN) and XhoI (Roche Diagnostics Corporation). The EcoRI site of the gene fragment was blunted by Klenow to facilitate cloning. The pcDNA3.1-Myc-RhoA plasmid was digested with NotI, treated with Klenow, and digested with XhoI to remove the RhoA gene. The two fragments were ligated overnight at 16°C and transformed into JM109. The resulting clones were verified by restriction mapping and automated sequencing.

CV-1 cells grown on 150 mm dishes to 50-80% confluency were transfected with the Myc-RhoGDIγ plasmid, the HA-RhoC plasmid, or both. Cell lysates were prepared by lysing the cells in IP buffer (50 mM Tris, pH 7.5, 150 mM NaCl, 1.5 mM MgCl2, 0.5 mM DTT, 20 mM ß-glycerophosphate, 1 mM sodium vanadate, 0.1% Triton X-100, and protease inhibitors) 42 hours post-transfection. HA-tagged RhoC was immunoprecipitated with the anti-HA affinity beads (Covance) and subjected to SDS-PAGE electrophoresis. Western analysis of Myc-tagged RhoGDIγ was performed using an anti-Myc antibody (Upstate) at a 1:1500 dilution in 5% milk-TBS-Tween.

3. Results

3.1. Validation of FRET detection in solution via FLIM

The FRET assay in solution (detailed under section 2.2), was used to validate the capability of the FLIM system of detecting FRET, as illustrated in Fig. 2(a). As shown in Fig. 2(b), the lifetimes of the substrate before and after cleavage were measured to be 1.79 and 2.45 ns, respectively. This is consistent with the fact that FRET decreases the fluorescence lifetime of the donor. The 50 ps lifetime discrimination of the FLIM system was adequate for detecting

#88805 - $15.00 USD Received 19 Oct 2007; revised 13 Dec 2007; accepted 14 Dec 2007; published 19 Dec 2007

the lifetime difference of 660 ps, before and after cleavage of the substrate. Moreover, the lifetime of the substrate after cleavage (2.45 ns), was confirmed to be similar to the lifetime of the product standard (2.42 ns), which represents complete cleavage of the substrate by the enzyme. This demonstrates the FLIM system's capability of detecting FRET in a well-controlled system. Because of the wide tunability of the dye laser, the FLIM system could be adapted to studies of ECFP (or Cerulean) and EYFP pairs in living cells.

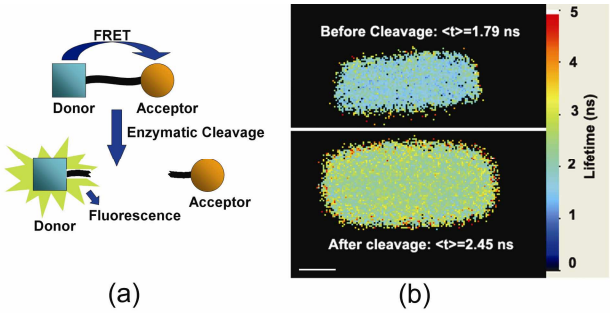

Fig. 2. FRET experiment in solution. (a) Concept of a FRET assay used to monitor cleavage of a peptide substrate consisting of a linked fluorescence donor and a quenching acceptor, (b) FLIM lifetime images of the donor before cleavage (upper) and after cleavage (lower). The scale bar represents 50 μm.

3.2. Lifetime measurements of intracellular ECFP

To ensure the reliability of the lifetime measurements of intracellular ECFP, several experiments were performed to verify the insensitivity of lifetime measurements to the effects of known artifacts, such as photobleaching, difference in plasmid uptake and expression, and variation in cell morphology.

To test if the experiments were subject to photobleaching, two consecutive measurements of ECFP fluorescence were taken on living cells to test the reproducibility of the measurements. The lifetimes of 4 cells transfected with ECFP-RhoGDIγ + EYFP and 5 cells transfected with ECFP-RhoGDIγ + EYFP-RhoC were reproducible to 1% and 0.02%, respectively, for the two measurements. However, the intensities of these two groups were only reproducible to 7% and 5%, respectively, for the two measurements. Therefore, lifetime measurements were much less affected by photobleaching than intensity measurements. We noted that although the intensities of all cells in a group decreased from measurement 1 to 2 due to photobleaching, the lifetimes of some cells in the group increased while those of others decreased, resulting in the high reproducibility of lifetimes shown above.

To examine the influence of difference in plasmid uptake and expression on measurement of each individual cell, intensity and lifetime of individual cells were compared. Fig. 3 shows ECFP fluorescence intensity image (a) and lifetime image (c) of living CV1 cells transfected with ECFP-RhoGDIγ + EYFP-RhoC. The intensity image and the corresponding histogram (b) show that the distribution of ECFP fluorescence within each individual cell was heterogeneous. Moreover, cells within a population had different fluorescence intensities. The lifetime image and the corresponding histogram (d), however, exhibit far smaller variability: the lifetime of ECFP fluorescence within each cell was more homogeneous that the intensity. Moreover, cells within a population had similar lifetimes.

#88805 - $15.00 USD Received 19 Oct 2007; revised 13 Dec 2007; accepted 14 Dec 2007; published 19 Dec 2007

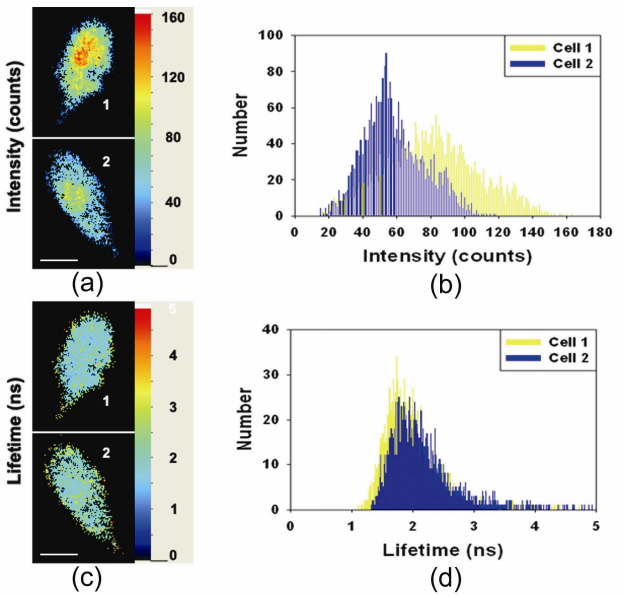

Fig. 3. ECFP fluorescence intensity (a) and lifetime (c) images of living CV1 cells transfected with ECFP-RhoGDIγ + EYFP-RhoC. The intensity image and the corresponding histogram (b) show that the distribution of ECFP fluorescence both within individual cells and within a population was heterogenous, making it difficult to interpret intensity-based FRET experiments. The lifetime image and the corresponding histogram (d), however, exhibit far smaller variability within individual cells and within a population, providing a sensitive method for detecting molecular binding events via FRET. The scale bar represents 20 μm.

Different cells in a sample might not be focused at the same optical plane due to differences in morphology, which might require adjusting focus for each cell during intensity-based measurements. We addressed this problem by intentionally changing the objective focus slightly in a controlled experiment to verify the relative insensitivity of lifetime measurements to small changes in focus. A slight change in focus caused 2%, 0%, and 6% variation in ECFP fluorescence lifetime, in contrast to 4%, 3%, and 26% variation in ECFP fluorescence intensity, for three living cells transfected with ECFP-RhoGDIγ + EYFP-RhoC.

#88805 - $15.00 USD Received 19 Oct 2007; revised 13 Dec 2007; accepted 14 Dec 2007; published 19 Dec 2007

3.3. Detection of molecular interactions via FLIM-FRET in living cells

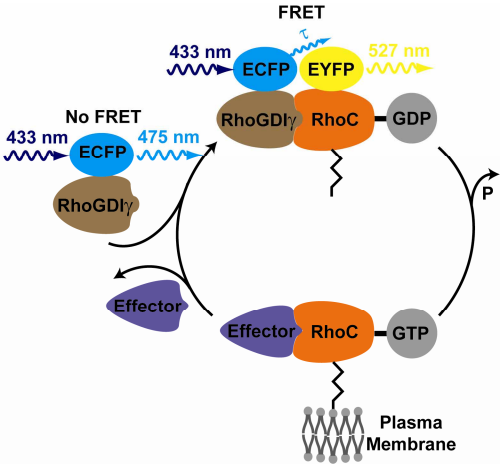

Fig. 4. Schematic depiction of FRET studies on RhoC and RhoGDIγ. Interactions between RhoGDIγ and RhoC would cause FRET to occur between fluorescent donor (ECFP) and fluorescent acceptor (EYFP). Excitation and emission maxima of ECFP and EYFP are labeled. Lifetime methods monitor the decrease of donor fluorescence lifetime (τ) to detect FRET.

Fig. 4 illustrates the experimental design for detecting the potential molecular interaction between RhoC and RhoGDIγ via FRET. Since RhoGDIγ and RhoC were attached to the FRET donor (ECFP) and acceptor (EYFP), respectively, their interaction would bring the FRET pair to close proximity. The resulting FRET phenomenon could then be detected with the FLIM system, because FRET decreases the fluorescence lifetime of the donor.

#88805 - $15.00 USD Received 19 Oct 2007; revised 13 Dec 2007; accepted 14 Dec 2007; published 19 Dec 2007

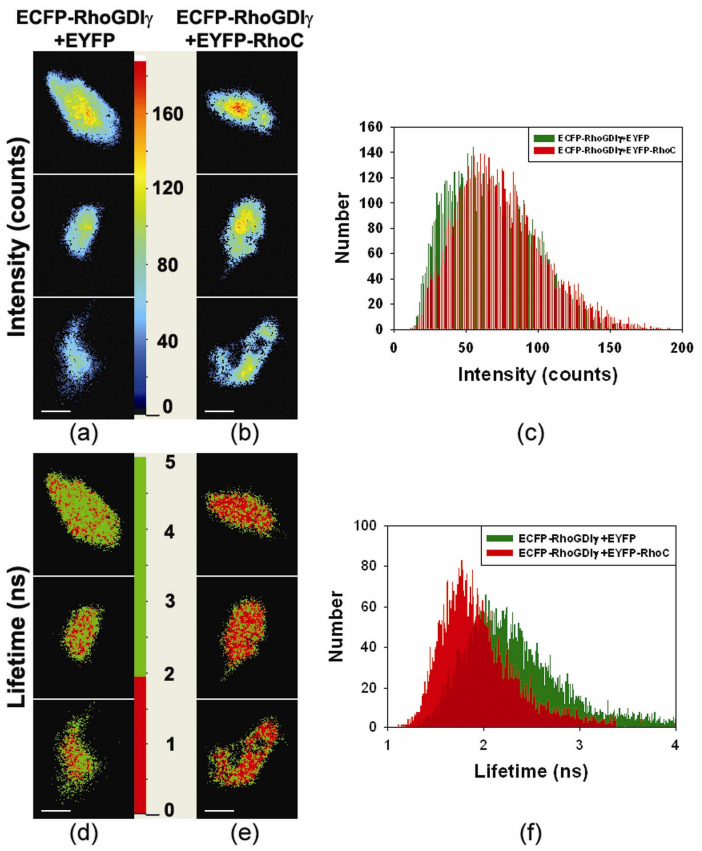

Fig. 5. ECFP fluorescence intensity ((a) and (b)) and lifetime ((d) and (e)) images of CV1 cells transfected with ECFP-RhoGDIγ + EYFP and ECFP-RhoGDIγ + EYFP-RhoC. The intensity images ((a) and (b)) show large variations in ECFP fluorescence intensity within each cell population, making it difficult to compare fluorescence intensity between different populations (c). The lifetime images of cells transfected with ECFP-RhoGDIγ + EYFP-RhoC (e) appeared redder than cells transfected with ECFP-RhoGDIγ + EYFP (d), suggesting that ECFP lifetime of the former was shorter than that of the latter. Histograms of lifetimes from these two populations of cells (f) confirmed that the mean lifetime of cells in (e) was shorter than that of cells in (d), indicating an interaction between RhoGDIγ and RhoC. The scale bar represents 20 μm.

In order to detect the interaction between RhoGDIγ and RhoC, two groups of cells (groups 1: transfected with ECFP-RhoGDIγ and EYFP; group 2: transfected with ECFP-RhoGDIγ and EYFP-RhoC) were studied, as the FRET between ECFP and EYFP occurring concurrently with interaction between RhoGDIγ and RhoC would cause ECFP fluorescence lifetime in group 2 to be decreased in comparison with that in group 1. Fig. 5 shows ECFP fluorescence intensity ((a) and (b)) and lifetime ((d) and (e)) images of CV1 cells transfected with ECFP-RhoGDIγ + EYFP and ECFP-RhoGDIγ + EYFP-RhoC. The intensity images ((a) and (b)) show large variations in ECFP fluorescence intensity within each cell population, making it nearly impossible to compare fluorescence intensity between different populations (c). In contrast, in the lifetime images ((d) and (e)), cells on the right appeared clearly redder than cells on the left, suggesting that ECFP lifetime of cells transfected with ECFP-RhoGDIγ + EYFP-RhoC was shorter than that of cells transfected with ECFP-RhoGDIγ + EYFP. Fig. 5(f) consists of histograms of lifetimes from these two populations of cells: ECFP-RhoGDIγ + EYFP (green) and ECFP-RhoGDIγ + EYFP-RhoC (red). The red histogram is shifted to the

#88805 - $15.00 USD Received 19 Oct 2007; revised 13 Dec 2007; accepted 14 Dec 2007; published 19 Dec 2007

left of the green histogram, showing that the mean lifetime of cells in Fig. 5(e) was shorter than that of cells in Fig. 5(d), and indicating an interaction between RhoGDIγ and RhoC.

Fig. 6 shows ECFP intensity (*left*) and lifetime (*right*) values of cells transfected with ECFP (*top*) and Cerulean (*bottom*) fusion plasmids. Group 1 (left box plot in (a) and (b)) consisted of 37 cells transfected with ECFP-RhoGDIγ and EYFP. This group was used as a negative control as no FRET between ECFP and EYFP would have occurred due to the interaction of RhoGDIγ and RhoC. Group 2 (right box plot in (a) and (b)) consisted of 60 cells transfected with ECFP-RhoGDIγ + EYFP-RhoC. Groups 3 and 4 (left and right box plots in both (c) and (d)) consisted of 30 cells transfected with Cerulean-RhoGDIγ + EYFP and 60 cells transfected with Cerulean-RhoGDIγ + EYFP-RhoC, respectively. The first quartile, the median, and the third quartile are shown within the boxes and the $10^{th}/90^{th}$ percentiles outside the boxes. All the plots are labeled with p-values of the Student's t-test, together with the mean intensity or lifetime value and standard deviation for each group of cells.

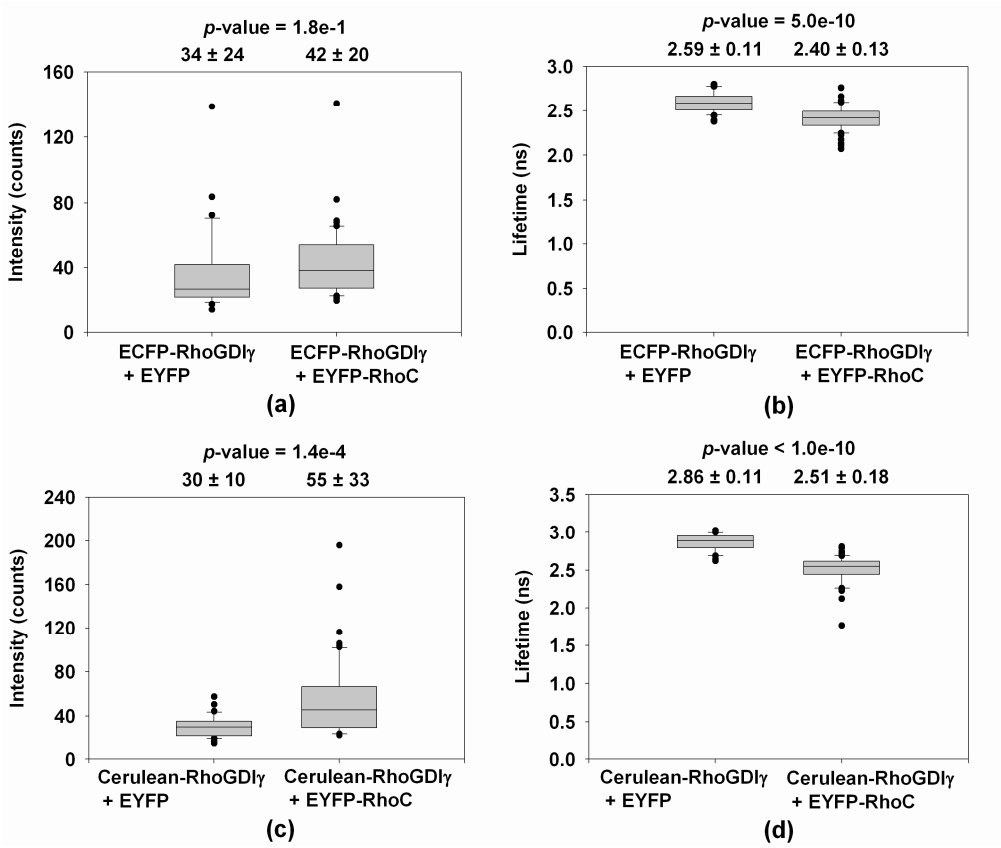

Fig. 6. ECFP intensity (*left*) and lifetime (*right*) values of cells transfected with ECFP (*top*) and Cerulean (*bottom*) fusion plasmids. Group 1 (left box plot in (a) and (b)) consisted of 37 cells transfected with ECFP-RhoGDIγ and EYFP. Group 2 (right box plot in (a) and (b)) consisted of 60 cells transfected with ECFP-RhoGDIγ + EYFP-RhoC. Groups 3 and 4 (left and right box plots in both (c) and (d)) consisted of 30 cells transfected with Cerulean-RhoGDIγ + EYFP and 60 cells transfected with Cerulean-RhoGDIγ + EYFP-RhoC, respectively. The first quartile, the median, and the third quartile are shown within the boxes and the 10th/90th percentiles outside the boxes. All the plots are labeled with p-values of the Student's t-test, together with the mean intensity or lifetime value and standard deviation for each group of cells. (a) and (c) Fluorescence intensities suffered from high variation within the cell population. (b) and (d) The FRET-induced decreases in lifetime (group 2 vs. group 1; group 4 vs. group 3) were statistically significant (p-value < 0.05)), indicating RhoGDlr-RhoC molecular interaction.

#88805 - $15.00 USD Received 19 Oct 2007; revised 13 Dec 2007; accepted 14 Dec 2007; published 19 Dec 2007

Fig. 6(a) and 6(c) show large variations of ECFP and Cerulean fluorescence intensity among cells within groups, making it difficult to interpret intensity-based measurement without lengthy calibration processes. In addition, the experimental groups often show higher mean intensities than those of the negative controls, probably due to higher transfection efficiency of ECFP or Cerulean vectors with weaker competitors in the experimental groups, since sizes of vectors can affect transfection efficiency [23]. Interaction between RhoGDIγ and RhoC is evidenced by the decrease of ECFP fluorescence lifetime in this experimental groups (group 2 and group 4), as compared to the corresponding negative control groups (group 1 and group 3), as shown in [Fig. 6(b) and 6(d)]. The difference in ECFP fluorescence lifetime is statistically significant, as confirmed by a Student's t-test with a p-value < 0.05.

3.4. Molecular interaction confirmed via biochemical assay

The interaction between RhoGDIγ and RhoC was subsequently confirmed using a biochemical assay. As shown in Fig. 7, western analysis of the Myc-tagged RhoGDIγ protein using an anti-Myc tag monoclonal antibody confirmed expression of the Myc-RhoGDIγ protein in CV-1 cells transfected either with the Myc-RhoGDIγ plasmid or with the Myc-RhoGDIγ and HA-RhoC plasmids. In comparison, CV-1 untransfected and CV-1 transfected with the HA-RhoC plasmids did not show any signal on the western blot probed with the antibody. The position of the band reacted to the anti-Myc antibody is located around 28 kDa, which is the expected size of the Myc-tagged RhoGDIgamma protein (Fig. 7).

Anti-HA affinity beads were used to immunoprecipitate the HA-tagged RhoC and its binding partners. Western analysis of the immunoprecipitates using the anti-Myc antibody showed very low levels of the Myc-RhoGDIγ protein associated with HA-RhoC from untransfected cells or from cells transfected with either the HA-RhoC or the Myc-RhoGDIγ plasmid (Fig. 7). On the other hand, the HA immunoprecipitate from CV-1 transfected with both Myc-RhoGDIγ and HA-RhoC plasmids gave a very strong signal of the Myc-RhoGDIγ protein (Fig. 7). This result independently demonstrates that RhoC and RhoGDIγ are able to interact with each other when they are co-expressed in CV-1 cells, yielding a stable complex that can be isolated and analyzed by western blot.

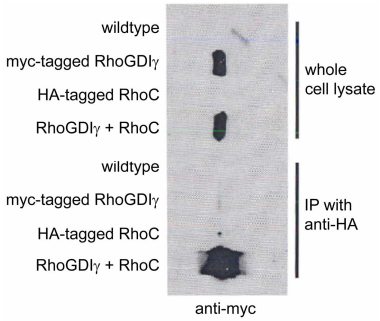

Fig. 7. Biochemical confirmation of RhoC-RhoGDIγ interaction. Immunoprecipitation of HA-tagged RhoC was performed using lysates of CV-1 cells transiently expressing Myc-RhoGDIγ, HA-RhoC or both. Untransfected CV-1 (wildtype) was included as a mock control. The immunoprecipitates (or whole cell lysates) were analyzed by immunoblotting with an anti-Myc tag antibody. The position of Myc-GDIγ is indicated.

4. Discussion

Fluorescence lifetime imaging microscopy (FLIM) offers an attractive means of performing FRET experiments with high spatial-sensitivity for subcellular molecular localization and binding studies in living cells, because it is independent of fluorophore concentration and artifacts, such as absorption and scattering, that affect intensity-based measurements [15, 17, 18, 21, 22]. We applied our unique UV-visible-NIR fluorescence microscope with 50 ps lifetime discrimination to the study of molecular interactions both in solution and of an

#88805 - $15.00 USD Received 19 Oct 2007; revised 13 Dec 2007; accepted 14 Dec 2007; published 19 Dec 2007

oncogene in living cells using FRET. We demonstrated the capability of our FLIM system to measure FRET via a well-established FRET assay (Fig. 2).

We then sought to study the interaction between RhoC and RhoGDIγ (Fig. 4), because very few reports of RhoC binding specificities to RhoGDI exist [40]. Previously, it was found that expression obtaining large amounts of recombinant RhoC protein in E.coli and other systems results in very low yield, thereby hampering the use of the traditional biochemical and biophysical methods to study the RhoC function due to difficulties in producing the wild-type recombinant protein [41]. In this report, we describe the first *in vivo* application of FRET to understand the regulation of RhoC activation by studying its binding to RhoGDIγ in living cells as a paradigm. This is a crucial step for the eventual evaluation of potential drugs aimed against the tumorigenic functions of RhoC.

Fluorescent proteins (FPs), including enhanced cyan fluorescent protein (ECFP) and enhanced yellow fluorescence proteins (EYFP), are used as the FRET pair in this study for the following reasons. First, they are well tolerated by biological systems, as demonstrated by healthy transgenic mice that express the FPs, making them suitable for experiments *in vivo* [42-44]. Second, they have no known intrinsic intracellular targets [45], suggesting they are unlikely to alter the endogenous biological functions of the experimental system. However, it is important to note that in some studies, the relatively large size of FPs was found to interfere with the molecular interactions of interest and cause false negatives [46]. Moreover, molecules that do not interact directly but become associated with a common partner can still produce positive FRET results [45]. Hence, as in this study, molecular interactions detected via FRET are often validated by other biochemical approaches.

Lifetime measurements of the fluorescence donors were found to be more reproducible, sensitive, and specific than intensity measurements. Lifetime values are much less likely to be affected by extraneous technical factors that strongly affect intensity-based measurements, including photobleaching, difference in plasmid uptake and expression, and slight change in focus (Fig. 3). Moreover, lifetime measurements of the fluorescence donors do not suffer from the recently reported problem of photoconversion of the acceptor, YFP, to a CFP-like species [47], which is encountered in acceptor photobleaching FRET experiments and can lead to false positives, although some other published results reported no such photoconversion under similar conditions, for reasons still under exploration [48, 49]. Hence, FLIM provides a sensitive method for detecting molecular binding events via FRET.

We detected the molecular interaction between RhoC and RhoGDIγ, as evidenced by the decrease in the fluorescence lifetime of the fluorescence donors (Fig. 5 and Fig. 6). The decrease in the fluorescence lifetime of Cerulean (350 ps) is greater than that of ECFP (190 ps), suggesting Cerulean as a better fluorescence donor because the FRET-induced fluorescence lifetime decrease of Cerulean would be less likely to be negated by other experimental variations. However, the 50 ps lifetime discrimination of the FLIM system used here was sufficient for detecting the lifetime decrease for both ECFP and Cerulean.

The measured lifetime values of the donor are consistent with those reported in the literature [38], though it is worth noting that measured lifetime values could vary from one report to another due to difference in FRET efficiency determined by the distance, orientation, and stoichiometry between interacting molecules as well as differences in instrumentation and data analysis. In our experience, even though the absolute lifetime values could vary by a few hundred picoseconds when different thresholds were used in the data analysis, the lifetime differences between the control and experimental groups always remained similar. Therefore, only comparison of absolute lifetime values taken with the same system gives meaningful information.

We noted that there was a distribution in donor lifetime within each group of cells, as illustrated by Fig. 6(b) and 6(d). This could be attributed to system noise, as well as to small variations between cells within each group. It is worth noting that in our system, lifetime of each cell was calculated as a mean value of a lifetime histogram for a ROI that enclosed the cell and consisted of thousands of pixels in the lifetime image. Hence, much of the effect of quantum noise is averaged out, as demonstrated by an example of two fluorescent samples

#88805 - $15.00 USD Received 19 Oct 2007; revised 13 Dec 2007; accepted 14 Dec 2007; published 19 Dec 2007

which differed only in the concentration: the histogram for a low concentration region was observed to have a broader distribution than for a high concentration region, but both regions had the same lifetime, which was calculated as the mean value of the distribution [30]. This is also illustrated in Fig. 3, in which the lifetime histograms of the two cells overlapped significantly despite the distribution of lifetime values within each cell (d).

We recognize that there might be subpopulations of 'unbound' donors, which decay at intrinsic lifetime, and 'bound' donors that decay at reduced lifetime due to FRET with the acceptor, which coexist in cell samples. Future work using multi-exponential models would allow us to quantify FRET efficiency by distinguishing these subpopulations [15]. As technology advances, better fluorescence proteins with improved quantum yield, higher extinction coefficient and single-exponential lifetime might be used instead of ECFP, Cerulean, and EYFP, for quantitative FRET studies [50-52].

The instrumentation and data analysis presented in this article can nonetheless be applied to detect the presence of molecular interactions of key oncogenes in living cells. This holds promise to provide, among other applications, a reliable method to test the molecular mechanisms of novel therapies against cancer targeted to specific molecular interactions.

Acknowledgments

This work was supported by a research grant from The Whitaker Foundation (M.-A. M. and S. D. M.), National Institutes of Health CA-112173 (M.-A. M. and S. D. M.) and CA 77612 (S. D. M.), Burroughs-Wellcome Fund (S. D. M.), the US Army Breast Cancer Research Program (S. D. M.), and Breast Cancer Research Foundation (S.D.M.).

#88805 - $15.00 USD Received 19 Oct 2007; revised 13 Dec 2007; accepted 14 Dec 2007; published 19 Dec 2007